Fundamental trade-off between speed of switching and robustness of genetic switches limits dynamic control of metabolism

Kaushik Raj[1], William T. Z. Wong[1], Beini Zhang[1], and Radhakrishnan Mahadevan[1,2,**]

[1]Department of Chemical Engineering and Applied Chemistry, University of Toronto, Canada
[2]Institute of Biomaterials and Bioengineering, University of Toronto, Canada
[**]Corresponding author, krishna.mahadevan@utoronto.ca

1 Abstract

Bi-stable gene regulatory motifs are found in a wide variety of natural gene regulatory networks and effect transcriptional switching between stable phenotypic states in cells. In synthetic gene regulatory circuits, these architectures can be leveraged to dynamically switch between distinct metabolic states for metabolic engineering and therapeutic applications. However, the lack of modularity and predictability of these motifs in varying environments has limited widespread application, especially since the factors that affect switching characteristics are still unclear. In this work, we use a mathematical model along with a newly developed dynamical modeling and continuity analysis framework to analyze the dynamics and robustness of bi-stable switches over a range of biologically relevant model parameter values. We identify a hitherto undiscovered fundamental trade-off between the robustness of the motif - the parameter ranges over which it retains bi-stable function, and the speed at which it effects a phenotypic change. Further, using *E. coli* as a model host, we constructed a large library (100) of transcriptional switches that show a wide range of switching speeds, to experimentally demonstrate the presence of this trade-off. The presence of this trade-off has significant implications on the design of transcriptional switches for diverse applications and explains the circuit architecture of naturally occurring transcriptional switches as well. Additionally, we anticipate that our diverse library of experimentally validated robust bi-stable switches will be valuable to effect phenotypic changes with differing switching speed requirements for metabolic engineering applications.

2 Significance statement

The ability to switch genes on and off in response to spatio-temporal stimuli is critical to the survival of all organisms. At the cellular level, such switching is effected by regulatory motifs such as the bi-stable genetic toggle switch. Bi-stable motifs also serve as a primitive mode of cellular memory - "remembering" the last environment to which the cells have been exposed. In this work, we uncover a fundamental trade-off between the robust functioning of these switches and the speed at which they can effect a change in the gene expression landscape. These findings have a broad impact on the design and use of such synthetic gene regulatory devices across several fields such as industrial biotechnology, healthcare, etc.

3 Introduction

Gene regulatory networks in cells confer them the ability to sense their environments and actuate an array of intracellular and extracellular transcription based responses such as the production of substrate assimilation machinery[1], initiating cell division[2], and fighting extracellular pathogens[3]. These networks can be decomposed into smaller sub-networks or motifs that are composed of a few parts and carry out specific functions[4]. One such motif is the bi-stable gene regulatory motif, which helps cells exhibit two distinct stable phenotypic states in response to environmental cues. It is considered to be a primitive form of cellular memory[5], since even the transient presence of inducer molecules can effect a stable change in the state of the motif. Such motifs are realized in the native gene regulatory networks of organisms using a double-negative feedback architecture (i.e. two repressors repressing each other's transcription from inducible promoters) or a positive auto-regulatory architecture (i.e. a transcription factor that induces its own production)[5].

Inspired by the design of the bi-stable lambda phage switch, the first synthetic bi-stable motif - the genetic toggle switch Figure 1 was constructed using a pair of repressors (lacI and cI) that inhibit each other's transcription and is considered to be a pioneering invention in the field of synthetic biology[6]. Since its conception, the genetic toggle switch, with modifications to its components has been employed in several bio-engineering applications, including in metabolic engineering to decouple growth and production metabolic states to improve chemical production[7,8], and in therapeutic applications to detect the presence of inflammation markers[9,10]. It has also been proposed as a solution for bio-containment of engineered microbes, designed to kill cells that are outside a contained environment[11,12]. The presence of two stable steady states reduces the amount and duration of inducer required to effect a response in the switch, making it a highly valuable induction system in noisy environments to reduce cellular heterogeneity.

However, despite these proof-of-concept applications, bi-stable motifs have not seen widespread use in scaled up chemical production or therapeutic applications. A major concern with employing this motif for diverse applications, is its context specificity and the lack of predictability of its functional range. Specifically, many versions of the switch have been shown to be bi-stable only in a narrow range of environmental conditions, becoming mono-stable when subject to perturbations in the growth conditions[6,14]. This precludes their successful deployment as memory elements that require transient induction. Additionally, since these switches use transcription - a relatively slow process in cells, the time taken to switch between the states can be quite large[7]. This impacts their use in metabolic engineering applications where a fast switch from growth to production stage may be necessary to realize optimal production rates of chemicals[15].

Previous studies examining the effects of the growth rates of the host organisms and the metabolic stresses inflicted on them have indicated that there is indeed an interplay between the the proper functioning of bi-stable circuits and the conditions in which the host organism is grown[16–18]. Specifically, a loss of bi-stability can result when the production of circuit proteins is unable to keep up with their dilution resulting from growth of the host organisms, or when cellular resources are not able to be effectively partitioned to produce the required amounts of circuit proteins due to cellular burden. Consequently, in order to alleviate this burden, there have been efforts to reduce the burden on host cells caused by the expression of the circuit proteins, while maintaining bi-stability[14]. The speed of switching between the two stable states is also an important characteristic that is often overlooked when designing the toggle switch. Fast acting switches can reduce the latency of engineered biological systems and could reduce

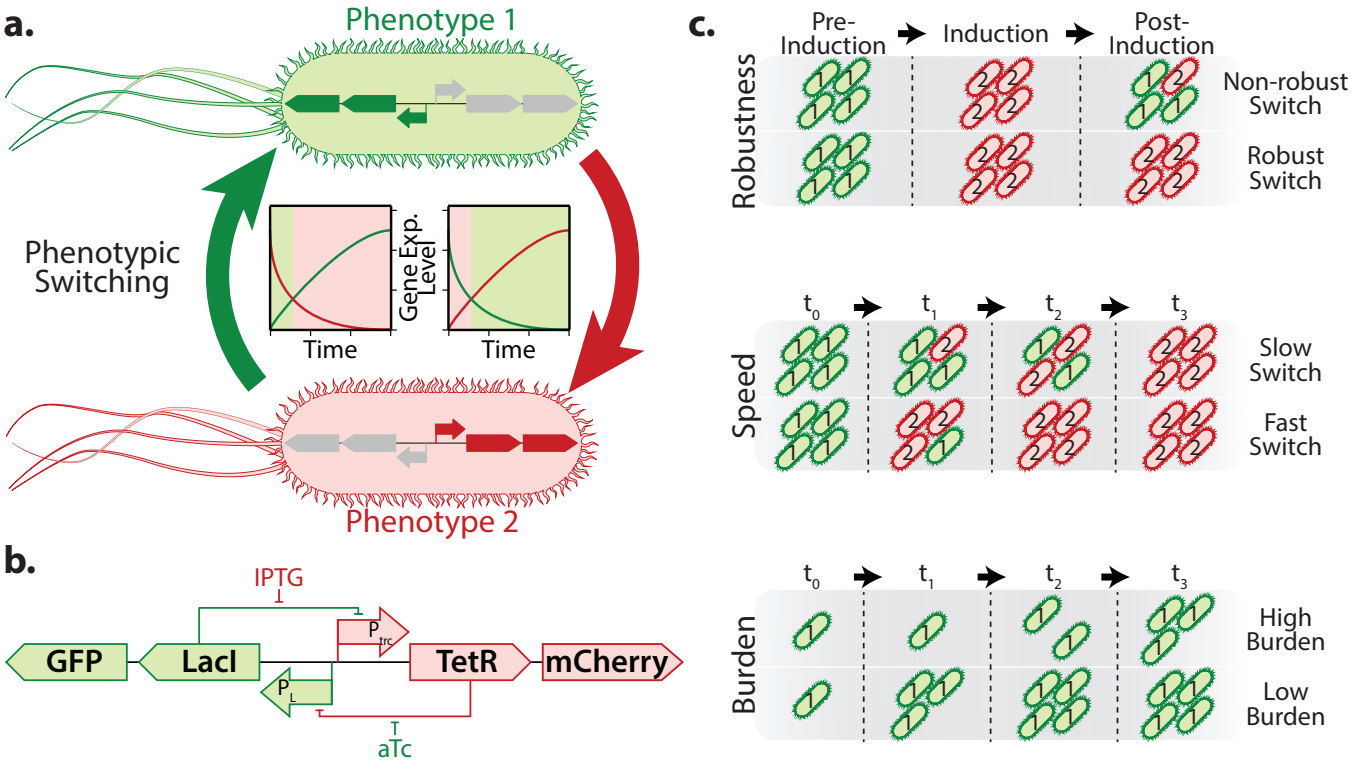

Figure 1: Phenotypic switching in cells and their important functional characteristics. a. Gene regulatory networks can be used to effect phenotypic switching in cells to make them express distinct sets of genes or entire pathways in response to stimuli, thereby conferring the cells with distinct phenotypes depending on the stimuli to which they are exposed. **b.** The genetic toggle switch (developed by Litcofsky et al[13]) is an example of a gene regulatory device which can enable host cells exhibit distinct stable phenotypes through a double negative feedback circuit where two repressors - TetR and LacI which mutually repress each other's production. We use the genetic toggle switch to study important functional characteristics of switches - illustrated in **c.** Specifically, we are interested in analyzing the effect of different switch constructs on **switch robustness** - the ability of cells to maintain their state even after the input signal is removed, **switch speed** - the speed at which the switch effects the change in phenotypes, and **switch burden** - the impact on cellular growth caused by expression of the switch's components.

inefficiencies in these systems - i.e. the less time spent in transition from one state to another, the less resources wasted in an undesirable metabolic state. This characteristic is highly desirable in microbial chemical production platforms, where a fast switch from a growth to a production phenotype is critical to make such bioprocesses economically feasible[15]. Hence, while designing bi-stable motifs for scaled-up platforms, the two characteristics - robustness to cellular resource availability and the speed of switching are very important to optimize.

In this work, we first developed a dynamical modeling framework to identify the effects of varying the parameters of a bi-stable motif model on its speed of switching and robustness to varying protein production rates, using the genetic toggle switch as a model circuit. Through simulations on our model using this framework, we observed that the speed of switching in a toggle switch can be improved by increasing the degradation rates of the repressor proteins in the system. However, this resulted in a decrease in the range of protein production rates over which the toggle switch remains bi-stable, indicating a trade-off between these two characteristics. Through a systematic analysis of the switching characteristics over

a range of biologically relevant parameter values, we identified optimal parameter ranges that result in maximal robustness of the toggle switch. To experimentally validate these findings, we then constructed a representative toggle switch with the repressor proteins coupled to a fluorescent reporter to enable live tracking of the switch's state. We then built a large variant library of our newly developed repressor-reporter fusion toggle switch, to validate the presence of the speed - robustness trade-off that was indicated by our models.

4 Results & Discussion

4.1 Model description and establishing switch function metrics

The mathematical formulation of the bi-stable architecture that we have proposed tracks the concentration of two repressors and consists of 8 parameters that are engineerable *in vivo*. Specifically, the repressor production rates - k_{p1}, k_{p2} can be altered by modifying the promoter or the ribosome binding sequence to enhance/inhibit transcription and translation rates. The co-operativity of the repressors - n_1, n_2 and their equilibrium dissociation constants - K_{diss1}, K_{diss2} can be altered by modifying the binding sites of the repressors to each other and to their promoter sites. The parameters K_{diss1} and K_{diss2} also signify the concentration of repressors at which their corresponding promoters result in half-maximal production of the other repressor. Finally, the repressor degradation rates - k_{deg1}, k_{deg2} can be increased by adding protease affinity tags to the terminii of the proteins. Among these parameters, the repressor protein production and degradation rates are the easiest to engineer due to the availability of a robust tool to calculate the strength of ribosome binding sites of any DNA sequence[19] and genetic parts that result in varying affinities to proteases[20]. The cooperativity of typically used repressors in synthetic bi-stable motifs - LacI and TetR is 2 and hence, the parameters n_1 and n_2 were set to this value for all our simulations. Additionally, we identified that for bioengineering applications, the speed of switching between the two states and the ability to retain bi-stable behavior in a range of different conditions that impact protein production rates, are two important characteristics of a desirable bi-stable motif. Hence, we wished to leverage our newly formulated dynamical modeling framework to examine the effects of varying the two engineerable parameters - protein production and degradation rates on these two functional metrics.

Studies have previously shown that protein production rates in cells are highly variable depending on the growth rate, which itself is governed by an array of environmental conditions to which cells are exposed[18,21]. Since our goal is to determine parameter ranges that result in functional bi-stable switches across a range of conditions, we define the robustness of the switch as its ability to retain bi-stable behavior in response to variations in protein production rates. Hence, for a given set of other parameter values, we evaluated the values of the repressor production rates k_{p1}, k_{p2} that serve as limit points - points that set the threshold for the motif switching from bi-stable to mono-stable behavior, by performing a two-parameter continuity analysis on the toggle switch model. All parameter values within the region bounded by the motif's limit points will result in a bi-stable configuration, while those outside are mono-stable. As a feasibility limit, we set 1000 µM/h as the maximum possible repressor production rate, which corresponds to a production rate of nearly 25% of the total cellular protein concentration being produced every hour[22]. We computed the robustness metric as the fraction of the area bounded by the bi-stable region in the protein production parametric space to the entire protein production parametric space (i.e. a robustness

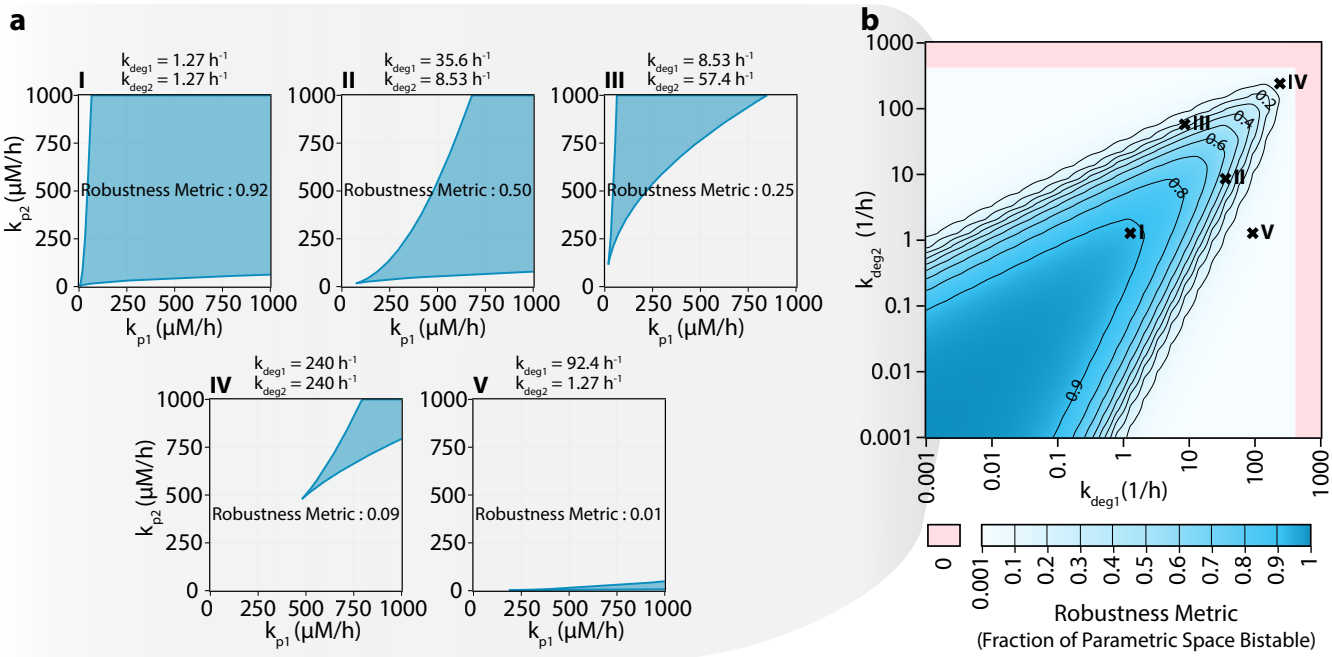

Figure 2: Determination of Robustness Metric: a. Robustness of the bi-stable motif to varying protein production rates. The region of bi-stability for a given set of parameter values can be obtained by performing a two-parameter continuity analysis on a dynamical model of the bi-stable motif. The area bounded within the shaded region corresponds to the range of repressor production rates where the system is bi-stable. The robustness metric is calculated as the fraction of the parametric space that is bi-stable. **b.** Robustness landscape over the entire range of experimentally realizable degradation rates. Continuity analysis on all combinations of feasible degradation rates of the repressor proteins was used to compute the robustness metric for each parameter set.

metric of 0.1 implies that 10% of all possible protein production rates will result in bi-stable behavior) (Figure 2a).

The speed of switching for a given set of parameters can be characterized by calculating the concentration of the two repressors over time upon the addition of inducers, simulated by altering the DNA binding affinities of the corresponding repressors (K_{diss1}, K_{diss2} set to infinity to simulate the higher affinity of repressors to inducer molecules than their DNA targets)[23]. In our simulations, the time taken to switch between states was determined as the the time taken for either repressor to reach 99.99% of their steady state concentrations Figure S1c, d. While the robustness metric directly incorporates all feasible production rates (k_{p1} and k_{p2}) into its calculation, the speed metric does not, and may vary within the parameter bounds set by our robustness calculations. Hence, we calculated the speed metric as the inverse of the average time taken to switch between the states using repressor production rates at the four extrema of the robustness metric curve (Figure S1). We observed that our speed metric is largely intransigent to variations in the repressor production rates, with deviations from the mean value limited to less than 5% for most cases analyzed (Figure S4).

4.2 Speed-robustness trade-off emerges in the toggle switch model

Having established standard metrics to evaluate the switch's function for a given parameter set, we wished to perform a preliminary analysis of our bi-stable motif's functioning for a test case where the equilibrium

dissociation constants K_{diss} for both repressors was set to 1 µM. This parameter value is consistent with *in vivo* observations made in previous studies for the Lac repressor and corresponds to roughly 600 copies of the repressor protein resulting in half-maximal repression of the cognate promoter in a single *E. coli* cell[24]. We computed robustness values for combinations of degradation rates of the repressor proteins spanning 6 orders of magnitude - ranging from 0.001 h^{-1} to 1000 h^{-1} (as feasibility thresholds for protein degradation rates, corresponding to a protein half-life of 693 hours and 2.5 seconds respectively) (Figure 2b). The robustness metric showed a decreasing trend with increasing degradation rates, with infeasible regions (where no bi-stable configurations were possible), at very high degradation rates (repressor half life <4 seconds). This is in line with observations made in a previous computational study examining this phenomenon[25]. Additionally, for each value of the protein degradation rate, the maximum robustness was observed when both repressors had the same degradation rate, with robustness values dropping drastically with imbalances in these rates.

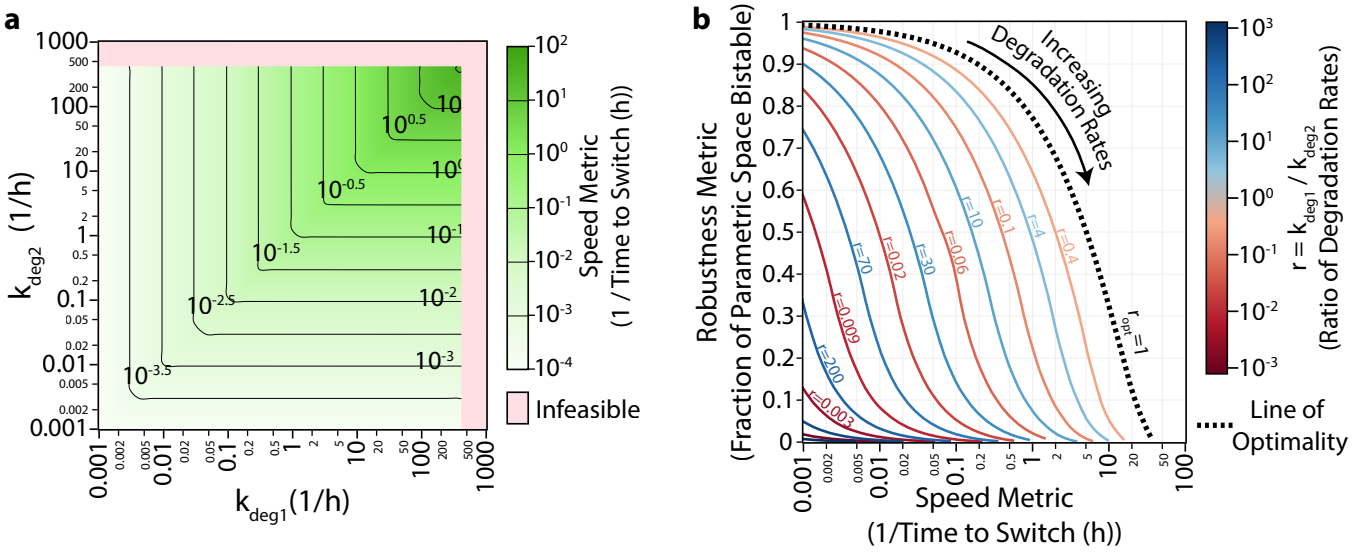

Figure 3: a. Speed metric landscape over the entire range of feasible repressor degradation rates for K_{diss}=1 for both repressors. **b.** Speed metric vs. Robustness metric for each ratio of repressor degradation rates with K_{diss}=1.

We observed that imbalances in the degradation rates of the repressors also resulted in impaired switching speeds (Figure 3a). However, in contrast to the trends observed for robustness, the speed of switching showed an increase (corresponding to a decrease in the time required to switch) with increasing degradation rates, reaching a maximum at the highest feasible combination of degradation rates. These results indicate that switches can be made faster through the addition of protease affinity tags, as suggested previously for a different switch architecture[26]. This observation further implies that there is a trade-off between the speed and robustness of the switch. Additionally, there is a maximum threshold on the speed of switching, which is determined by the maximal feasible value of the degradation rates, as determined from the robustness calculations.

In order to better understand the relationship between the two switch metrics, we plotted the robustness and speed metric values arising from all of our parameter sets (Figure 3b). We observed that for any given ratio of degradation rates (denoted 'r') of the two repressors, the speed and robustness metrics show a clear trade-off - as the speed metric increases, the robustness metric drops which can be realized by moving along

the lines depicted in Figure 3b. Interestingly, there is an optimal value of 'r' that forms an upper bound for the maximal robustness for any given switching speed and this value for our preliminary parameter set is 1 - where, the degradation rates of the two repressors are equal.

Following this, we wished to examine the trends in robustness and switch speeds over the entire range of feasible parameter values. Keeping the co-operativity at 2, we varied the equilibrium dissociation constants of the repressors over 5 orders of magnitude ranging from 0.005 µM to 500 M (corresponding to 3 copies and 300,000 copies of the repressor protein respectively in each cell, assuming the same volume as *E. coli*). This upper bound on the K_{diss} values represents approximately 10% of the cell's entire protein budget[22]. We find that the robustness landscapes across all parameter sets show the same decreasing trend with increasing protein production rates as observed in our preliminary parameter set (Figure S2). However, in contrast to our preliminary parameter set, we observed that the robustness and consequently, the range of feasible degradation rates and becomes smaller with increasing K_{diss} (which represents impaired repression by the repressor). These results indicate that a bi-stable motif that employs repressors with enhanced DNA binding ability will result in a highly robust construct and therefore, would allow for better tuning of the switch speed through the addition of protease affinity tags than similar motifs that use weakly binding repressors or those with leaky expression. While the robustness metric showed significant differences with changing K_{diss} values, the speed metric remained constant over the entire range of K_{diss} values, with only the feasibility region becoming smaller with poorer repressor-DNA binding (Figure S3). Along with our previous observation that the switch speed does not change with repressor production rates, this result indicates that the only parameter in our model that affects the switch speed significantly is the degradation rate of the repressor proteins, further demonstrating the importance of using protease affinity tags to accelerate bi-stable motifs.

Interestingly, upon analyzing the speed-robustness relationship for all combinations of K_{diss} values, we observed that the optimal ratio of degradation rates (r_{opt}) that resulted in maximum robustness at a given speed metric of the switch, changed with different combinations of K_{diss} values (Figure 4). Specifically, when the values of the dissociation constants for the two repressors remained equal, the r_{opt} was equal to 1. As the dissociation constants of the two repressors change, the r_{opt} changes correspondingly, seemingly trying to restore the imbalance caused by different binding affinities of the two repressors to their cognate promoter targets. This finding is very important while designing bi-stable motifs with two different repressors as in the case of the genetic toggle switch, in order to determine the optimal protease tag to add to each repressor.

4.3 Repressor-reporter fusion to characterize switch state in real time

Following the discovery of design guidelines to build better bi-stable motifs, we wished to validate our model findings by building faster switching variants of the genetic toggle switch described by Litcofsky et al[13]. Additionally, we also wanted to demonstrate the presence of a speed-robustness trade-off experimentally. In order to monitor the speed of switching, it is necessary to track the concentrations of the repressor proteins *in vivo* to determine when a state change has occurred. However, in the original design of the toggle switch, the repressor and fluorescent reporter proteins are de-coupled, precluding a quantitative analysis of repressor concentrations by simply measuring the fluorescence intensities of the reporters. Hence, we aimed to construct a fusion variant of the genetic toggle switch where the repressor and reporter proteins are

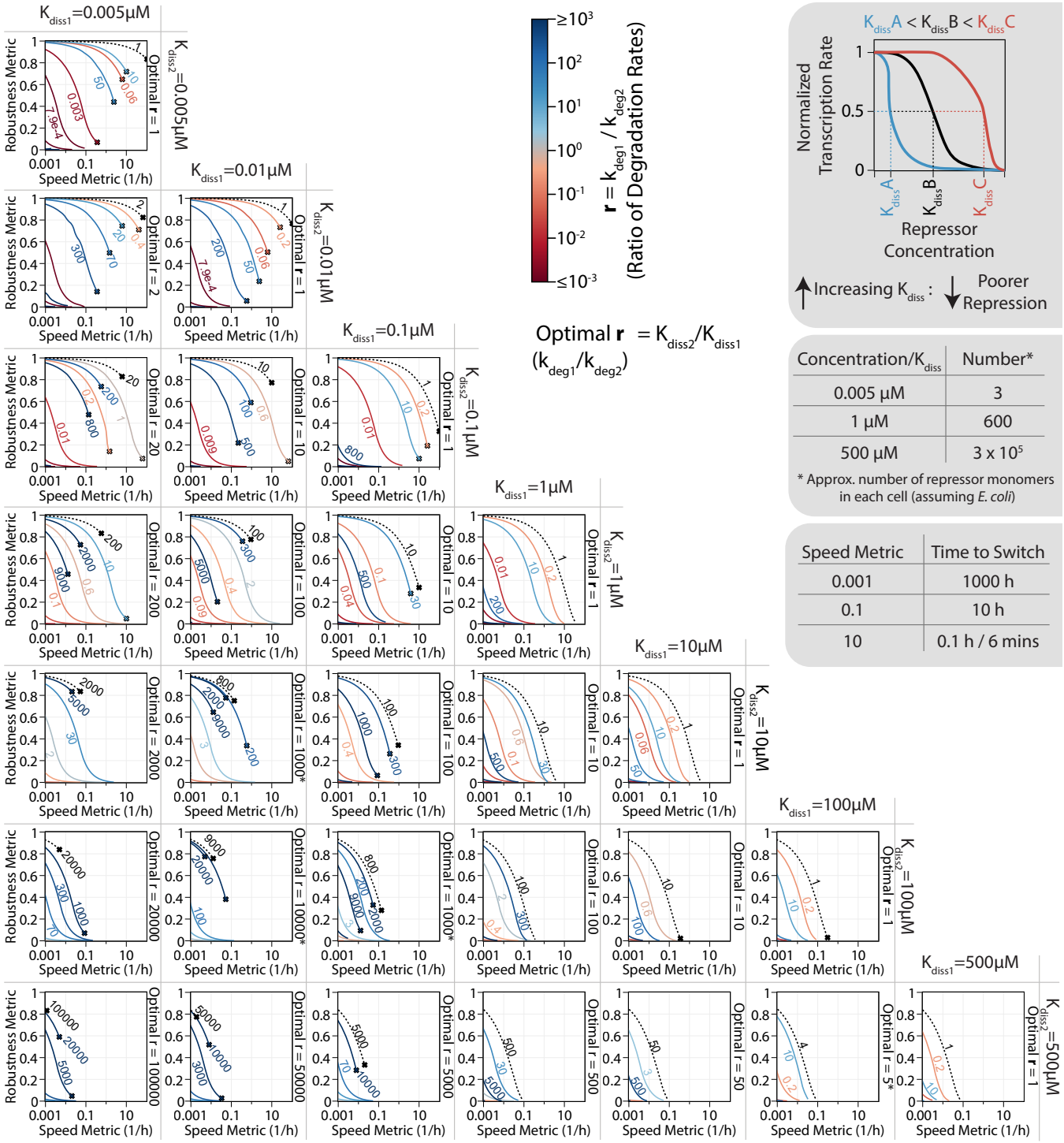

Concentration/K_{diss}	Number*
0.005 μM	3
1 μM	600
500 μM	3×10^5

* Approx. number of repressor monomers in each cell (assuming *E. coli*)

Speed Metric	Time to Switch
0.001	1000 h
0.1	10 h
10	0.1 h / 6 mins

Figure 4: Relationship between the speed metric and robustness metric over entire feasible parametric range. The relationship between the speed and robustness metrics plotted for all combinations of K_{diss} values that represent the physical limits of experimentally observable values for the parameter. The shaded boxes to the top-right illustrate the physical significance of the parameter - K_{diss}.

physically coupled to each other by means of the flexible protein linker - $(GGGGS)_2$[27]. In order to determine the optimal configuration of the repressor-reporter fusions (N-terminal vs C-terminal fusions) that resulted in similar repression characteristics as their non-fusion counterparts, we constructed all possible variants of

fusion constructs of the LacI repressor with the fluorescent protein GFP, and the TetR repressor with the fluorescent protein mCherry. We then inserted these constructs into test circuits where they would repress expression of a fluorescent protein and can be induced with their cognate inducer (IPTG for LacI and aTc for TetR). The test circuits used for each repressor, shown in Figure 5 consist of GFP or mCherry under the control of either the p_L or $pTrc$ promoter respectively. The fusion constructs with TetR or LacI were expressed constitutively as required in the test plasmid constructs, repressing production of the fluorescent reporters GFP and mCherry, until they are sequestered through the addition of aTC or IPTG respectively..

In our designs, we observed that neither configuration for both repressors resulted in a significant increase in leaky expression (expression of downstream genes without the addition of inducers) from their target promoters, indicating that the fusion constructs are at least as good as their wild-type counterparts in DNA binding ability (Figure S6). Additionally, we also examined the ability of the repressors to be induced by their corresponding inducer molecules. In all cases, the fusion constructs showed weaker induction characteristics than their wild-type counterparts, with higher concentrations of inducer being required for an equivalent de-repression of their promoters. We chose the fusion protein configuration that had a lower K_M (inducer concentration required for half maximal expression) and lower variance in induction characteristics. Hence, the TetR-mCherry (TetR at N-terminus and mCherry at C-terminus) and GFP-LacI(GFP at N-terminus and LacI at C-terminus) fusion proteins were chosen as optimal constructs for further experiments.

4.4 Constructing and characterizing a diverse toggle switch library

Having determined the optimal configuration of fusion proteins to ensure that the DNA binding and inducer binding abilities of repressor proteins are minimally affected, we assembled our representative toggle switch using GFP-LacI and TetR-mCherry as the repressors, with the ribosome binding strength of either repressor engineered to mimic the values found in the original pKDL071 version of the toggle switch [13] (shown in Table S1). Our fusion toggle switch functioned as expected, displaying high mCherry fluorescence (and correspondingly high TetR concentrations) when grown on IPTG and high GFP fluorescence (and correspondingly high LacI concentrations) when grown on aTc (Figure S7). However, the construct seemed to have lost bi-stability, reverting to a TetR high state after the removal of aTc, resulting in mono-stable constructs. This is possibly due to variations in the protein production rates effected by the calculated RBS values resulting in imbalances in the switch. Nevertheless, we used this construct as starting point to construct our variant library, since we would be able to restore bi-stability by altering the RBS strengths if our model predictions are accurate.

Next, we designed variants of the fusion toggle switch with varying ribosome binding site(RBS) strengths and protease affinity tags to create constructs that result in a range of protein production and degradation rates, as required to validate our model findings. To this end, we designed RBSs that we expected to show between 2 and 30 times the strength of the RBS in the original toggle switch - pKDL071 using the RBS calculator (v2.1) [19] (Table S1). In order to vary the degradation rates of the toggle switch proteins, we leveraged the native *ClpXP* protease in *E. coli* by tagging the repressors with the SsrA tag and its variants that have been used in previous studies to show graded degradation rates [20,28]. A list of RBS strengths and degradation tags we chose for each repressor are shown in Figure 5. This resulted in 20 variants of each fusion repressor, composed of all possible combinations of the RBSs and degradation tags.

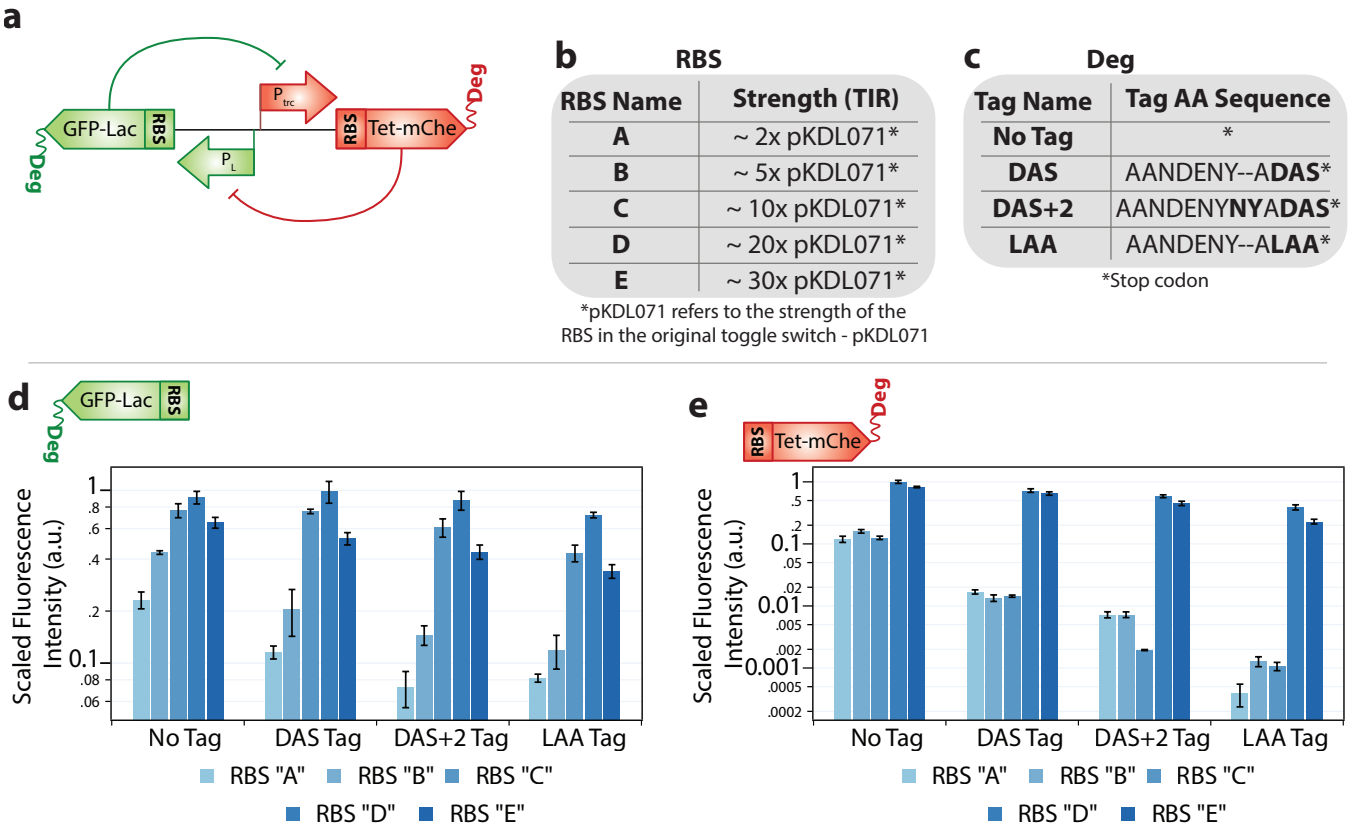

Figure 5: Fusion Toggle Switch Study Speed-Robustness Trade-off. a. An illustration of the fusion toggle switch with GFP-LacI and TetR-mCherry with modified ribosome binding site (RBS) and added degradation tags. **b.** The five RBS strengths (as predicted by RBS calculator v2.1[19]) chosen for each repressor relative to its value on the original pKDL071 toggle switch designed by Litcofsky et al[13]. The queries and translation rates corresponding to each RBS level is shown in Table S1. **c.** Degradation tags and their amino acid sequences added to the repressors for toggle switch library construction. Modified versions of the SsrA degradation tag that show different degradation rates were chosen. **d.** GFP-LacI and **e.** TetR-mCherry fluorescence intensities determined for each of the 20 RBS-degradation tag combinatorial variants of repressor-reporter fusion proteins, organized by the degradation tag used.

To shortlist functioning RBS and degradation tags for our final combinatorial library, we first examined the protein production and degradation rates of the 20 variants of each fusion repressor leaving the other repressor unchanged (40 constructs in total), by transforming plasmids harboring these constructs into *E. coli* MG1655 (ΔlacI) and inducing their expression with IPTG or aTc. We then monitored the levels of repressor proteins produced by the RBS-degradation tag combinations by recording the fluorescence intensity of the reporter attached to them. As expected, the addition of degradation tags resulted in progressively higher rates of degradation of the repressors and consequently, lower steady state fluorescence intensities from the reporter attached to them (Figure 5d, e and Figure S8). Furthermore, the strengths of the degradation tags indicated by these results are largely in line with observations made in previous studies ('LAA' has the highest strength, followed by 'DAS+2' and then 'DAS')[28]. The relative rates of degradation, as indicated by the reduction in the steady-state fluorescence intensity at each RBS level were estimated and have been listed in Table S2 and Table S3.

However, RBS strengths did not conform with our design parameters, specifically for TetR-mCherry, with many RBSs constructs showing minimal variation (Figure 5d, e and Figure S8). Hence, we shortlisted 10 combinations of RBS-degradation tag variants for each repressor, that showed the largest variability in the fluorescence intensities (and consequently the repressor production/degradation rates) in order to obtain a highly variable combinatorial library of toggle switch variants and thereby examine a large portion of the design space. We then constructed plasmids containing all possible combinations of the variants using the ligase cycling reaction method[29], sequence confirmed the 100 resulting plasmids, and transformed them into *E. coli* MG1655 (ΔlacI) for final characterization.

4.5 Switch variants show a wide range of switching speeds

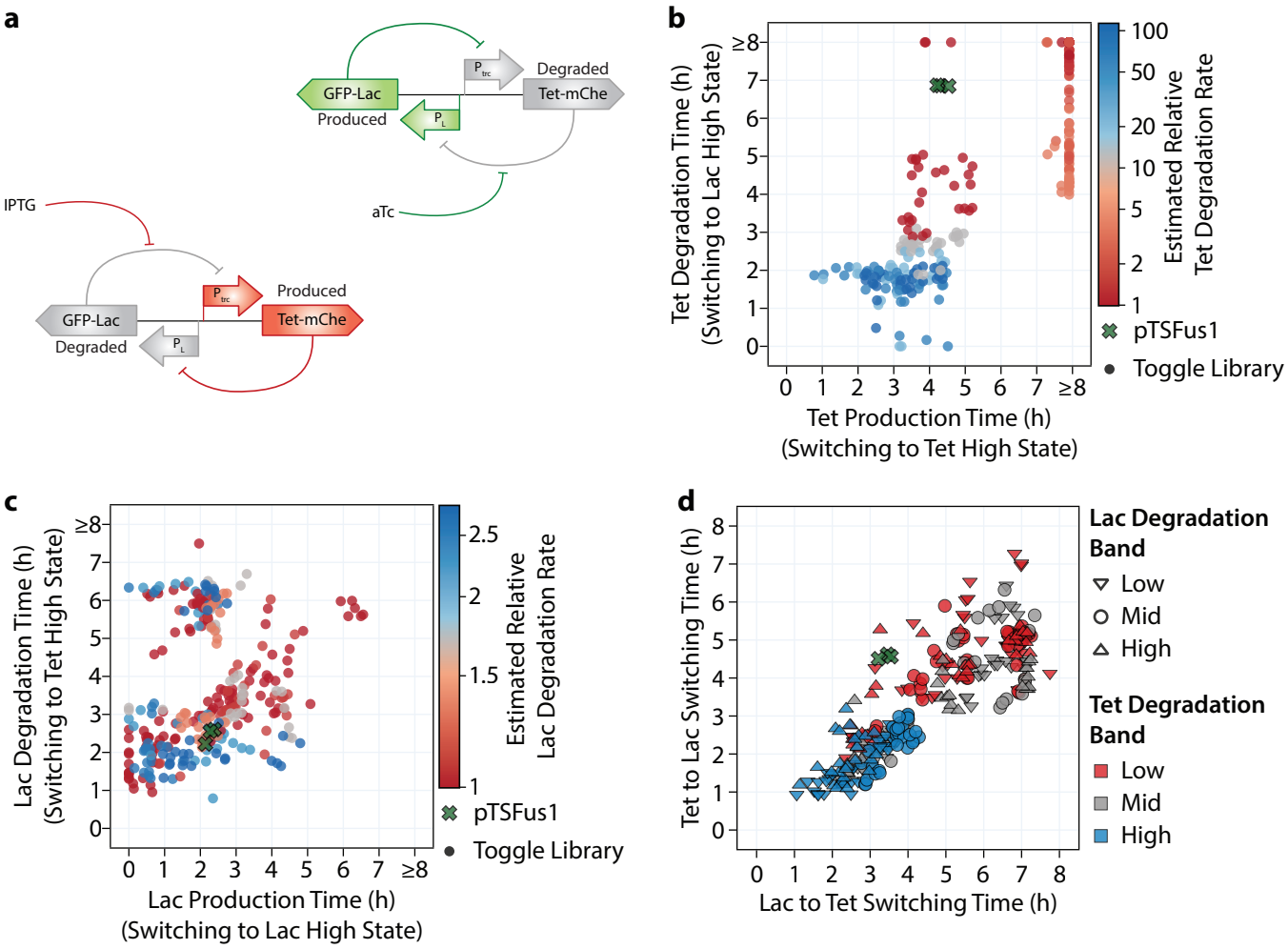

Figure 6: Switching time vs Degradation rates. **a.** Illustration showing the addition of different inducers and which repressors are produced or degraded in each case. The time taken by either repressor to be produced and degraded in the appropriate state is calculated. **b.** Effect of degradation tags on the Tet repressor in reaching steady state concentrations. **c.** Effect of degradation tags on the Lac repressor in reaching steady state concentrations. **d.** Effect of degradation tags on the switching time(calculated as the average of the time taken to produce and degrade the appropriate repressor for each state), with strains classified based on degradation levels estimated in Table S2 and Table S3

Leveraging our previously described high-throughput phenotyping platform[30], we examined the switch-

ing speed of our 100 switch variants in triplicate. We monitored the time taken by either repressor to reach its steady state maximum and minimum upon the addition of the corresponding inducer (Figure 6a). As expected, adding degradation tags and thereby increasing the degradation rates of the Tet repressor resulted in a generally faster rate of the Tet repressor reaching its steady state value in both states. In particular, the addition of degradation tags greatly reduced the time taken to degrade TetR from cells that are switching into the Lac high state, as indicated by the large reduction in the Tet degradation time for our library variants compared to the original construct (Figure 6b). We observed a similar trend with the Lac repressor as well, with many library variants with degradation tags showing a shorter time to reach the steady state value (Figure 6c). There were however, some Lac repressors with relatively low degradation rates (as predicted in Table S2 and Table S3) that reached steady state much faster than those with higher degradation rates, possibly due to their extremely low RBS levels, resulting in very small steady state values.

Nevertheless, upon comparing the effect of various degradation rates on the overall switching time (mean value of the time taken to degrade one repressor and produce another), we found that those constructs with higher degradation rates, generally resulted in faster switching to either state (Figure 6d) as predicted by our model. Specifically, we found that the degradation tags on the Tet repressor are highly effective in mediating a faster switch, likely due to the higher relative degradation rates in the Tet repressor than the Lac repressor (Table S2 and Table S3). However, in contrast to our model predictions, several constructs with intermediate degradation rates resulted in very slow switching. Upon a closer analysis, we found that these were constructs with extremely high protein production rates, which resulted in very slow growth and consequently, slower switching than even those constructs without degradation tags. This can be clearly seen when the switching times are plotted against the growth rates of the corresponding cells, where a number of variants with intermediate degradation rates result in very slow growth and therefore slow switching (Figure S9). A principal component analysis performed on these metrics also confirmed this observation, showing a strong negative correlation between the time taken to degrade repressor proteins and the host strain's growth rate for either state(Figure S10c). In other words, constructs with intermediate degradation rates resulted in slow switching only when the growth rate was low (Figure S10a, c). Hence, the growth rate of the resultant strains is an important parameter that also needs to be considered while designing switches. Regardless, our variant library consists of switches that show a wide range of switching time, many of which are faster than the initial construct, indicating that varying the degradation rates is indeed an effective strategy to alter switching speeds. Furthermore, we generally observed that higher degradation rates result in faster switching when the growth rate is constant (Figure S9 and Figure S10).

4.6 Trade-offs in switch function - experimental validation

Having confirmed the effect of adding degradation tags on the speed of switching, we examined the ability of our switch variants to retain their state after removal of their corresponding inducer i.e. the ability to maintain high levels of Tet after IPTG is removed and maintain high levels of Lac after aTc is removed. Based on their ability to retain their state after three consecutive transfers with no inducer, we classified the individual experimental replicates as - Bi-stable when both states are stable, Mono-stable when only either one of the Tet or Lac state is stable and unstable when the construct is unable to retain either state (Figure 7a). Our results show that a majority of strains with slow degrading repressors are bi-

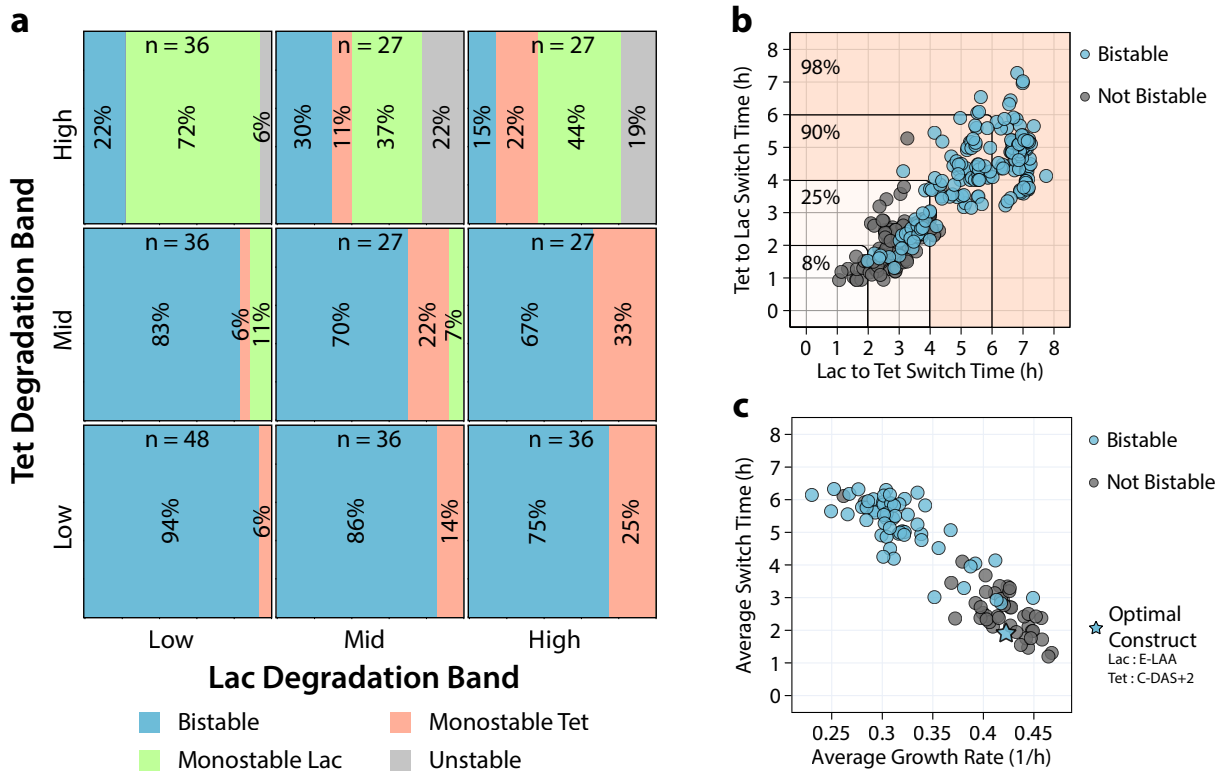

Figure 7: Trade-offs in toggle switch behavior: a Effect of varying degradation levels of the Lac and Tet repressor on the bi-stability of individual replicates. The percent of bi-stable, mono-stable and unstable constructs are shown within the boxes representing each degradation level combination. Constructs were classified into different degradation levels as shown in Table S2 and Table S3. Overall data for each construct is shown in Figure S11. **b.** The Lac state and Tet state switching times for individual replicates, classified based on stability. The percent of bi-stable replicates at each level of Tet and Lac switching times is shown within the plot. Overall data for each construct is shown in Figure S12. **c.** A trade-off between the average switching time (calculated as the average of the two state-switching times) and the growth rate of the each strain, classified based on stability. Constructs were designated bi-stable if all individual replicates were bi-stable. Individual replicate data shown in Figure S13.

stable, with the proportion of bi-stable strains decreasing as degradation rates are increased. We find the lowest proportion of bi-stable strains in the constructs with the highest degradation rates on both repressors. This is in remarkable agreement with our model findings where robustness (i.e. the region of bi-stability and consequently the number of bi-stable constructs) decreased with increasing degradation rates. Additionally, we also found that increasing the degradation rate of one repressor resulted in more constructs becoming mono-stable towards the other. Additionally, imbalanced degradation rates also resulted in lower robustness, as predicted by our model. We observed the same trends when the experimental replicates of each strain were combined to obtain the overall bi-stability of a construct as opposed to the individual replicates (Figure S11).

Next, we compared the number of bi-stable strains at each level of switching speed to study any possible correlations between the robustness and the speed metric. Once again, in remarkable agreement with our model predictions, we found a monotonically decreasing trend in the proportion of bi-stable constructs, with increasing switching speeds (or decreasing switching times) (Figure 7b and Figure S12). This confirms the presence of a trade-off between the switching speed and robustness in the genetic toggle switch, indi-

cating the need to carefully design switches with appropriate protein production and degradation rates. Importantly, we identify a range of different switch constructs that are fast switching while still being bi-stable. Additionally, since we uncovered previously that the growth rate of the host varies significantly depending on the switch configuration and fast growth is a highly desirable characteristic in metabolic engineering applications, we wished to identify optimally performing switch constructs that switch fast and remain bi-stable, while not imparting a severe growth burden on the host. Comparing the switching time, growth rate and the bi-stability of each strain, we found that all replicates of the construct with the 'E-LAA' Lac repressor and the 'C-DAS+2' Tet repressor resulted in optimal characteristics and can be investigated for further improvement (Figure 7c and Figure S13).

5 Conclusions

Gene regulatory circuits enable highly effective control of cellular states in engineered bacteria by modifying environmental conditions or through the addition exogenous chemical signals. This allows engineered cells to act as microscopic controllers - sensing their environments and actuating an appropriate genetic response. Such systems show immense potential for use in metabolic engineering and therapeutic applications. Specifically, bi-stable motifs can greatly reduce variability in cellular phenotypes by forcing cells to exist in one of two stable steady states. However, the design of such systems has been a difficult endeavour in the past due to an incomplete understanding of how each part of the circuit affects its function.

In this work, we have seen here that the design choices made during the construction of bi-stable motifs impacts their function to a great extent. Using a mass-action kinetics based model of the toggle switch, we have established a fundamental trade-off between the speed and robustness of bi-stable motifs. Additionally, we have also uncovered ways to engineer the toggle switch to accelerate the switching between the states. Specifically, in metabolic engineering applications, the time at which microbes are switched from growth to production phenotypes and the duration of the switch play an important role in determining the economic feasibility of the bioprocess. A slow switch to the production stage could result in impaired chemical production, which could in turn deem such processes economically infeasible.

While fast acting switches are highly desirable for metabolic engineering and other applications, we uncovered the presence of a trade-off between the speed of switching and the robustness of bi-stable motifs to varying protein production rates. This is a key trade-off that puts an limit on how much the speed of switching can be improved before resulting in instability. Alternatively, this finding also suggests that for applications where high robustness is required, slow acting switches are more preferable. Additionally, we also observed that while switches that employ higher degradation rates can be made bi-stable by increasing the production rates of the repressors that mediate the switch, this causes a growth burden on the host cell and that impacts the speed of switching. Conversely, strains that grow extremely fast also result in unstable bi-stable motifs. These three quantities - robustness, switching speed, and host cell growth-rate are therefore at odds with each other and the key to constructing optimal switches lies in carefully negotiating the effects of changing the switch's components on these three characteristics. We believe that these findings will be influential in designing bi-stable motifs for metabolic engineering and therapeutic applications. Moreover, our generalized dynamical model analysis framework can be used to analyze other regulatory motifs and could be a very useful tool in designing complex biological circuits. Further, we constructed a modified fusion variant of the toggle switch that uses repressor proteins that have fluorescent

reporters attached to them. This modified toggle switch could serve as an invaluable tool in dynamic control applications since the state of the switch can be readily determined by simply monitoring the fluorescence of the cells, in a non-invasive manner.

In this study, there were several constructs in the highest degradation band that were not bi-stable or mono-stable in either state (Figure 7a). This deviates from our predictions since based on our deterministic model, toggle switch constructs can be either bi-stable or mono-stable in one state. Stochastic effects where a change in switch state effected by noise in the system could explain this and should be considered in future modeling efforts. Furthermore, the effects of the growth rate of host cells on circuit function and vice versa should be explored further by using models of cellular resource allocation to predict growth rates when heterologous proteins are expressed in host cells. One potential way to alleviate the burden of expressing the toggle switch proteins is to build a variant library in a single copy vector or through genomic integration of the circuit as shown in a recent study[14].

Nevertheless, our combinatorial library of toggle switch variants show a wide range of switching speeds while remaining bi-stable and could be used to enhance the production of a diverse range of target compounds by decoupling growth and production phenotypes. We anticipate that this work will encourage the widespread use of bi-stable motifs in bioengineering for dynamic control of metabolism.

6 Methods

6.1 Mathematical model

The genetic toggle switch was chosen as the model circuit to study the effect of bi-stable motifs. It consists of two repressors that inhibit each others' transcription, resulting in a net positive feedback motif (Figure 1). The state of the switch can be altered by means of external inducers, which act by binding to and inactivating their corresponding repressor targets. The proposed mathematical model for the genetic toggle switch (shown in Eq. 1) was generated using mass action kinetics where $Repressor1$ and $Repressor2$ represent the repressors LacI and TetR in the case of the genetic toggle switch. For the sake of simplicity, we assumed that repressors binding to their cognate promoter targets occurred at a much faster time-scale than the production of the repressor proteins, thereby resulting in an equilibrium between the repressors and their targets. Additionally, we assumed that the rate of transcription and translation can be represented by a lumped parameter (k_p), distinct for each repressor but does not change over the course of the simulation. To simulate the effect of the addition of inducer molecules, the ability of the repressor species to bind to their cognate promoter targets was impacted by increasing the values of the parameter K_{diss} to a very high value, where the repressor could no longer inhibit gene expression from its promoter target.

$$\frac{d[Repressor1]}{dt} = \frac{k_{p1}}{1 + (\frac{[Repressor2]}{K_{diss2}})^{n2}} - k_{deg1} * [Repressor1] \quad \text{(Eq. 1a)}$$

$$\frac{d[Repressor2]}{dt} = \frac{k_{p2}}{1 + (\frac{[Repressor1]}{K_{diss1}})^{n1}} - k_{deg2} * [Repressor2] \quad \text{(Eq. 1b)}$$

where

$[Repressor1], [Repressor2]$: Concentration of repressors (μM)

k_{p1}, k_{p2}: Production rate of repressors ($\mu M/h$)

K_{diss1}, K_{diss2}: Equilibrium dissociation constant for repressors binding to cognate promoters (μM)

n_1, n_2: Cooperativity of repressor binding

k_{deg1}, k_{deg2}: Degradation rate of repressors (h^{-1})

6.2 Dynamical modeling framework

In order to systematically evaluate the effects of perturbing the model parameters on the switch's function, we formulated a general dynamical modeling framework that accepts as its inputs, an ordinary differential equation model of any gene regulatory motif or more generally, dynamical process. Following this, given a set of parameter values, our modeling framework calculates all the stable and unstable steady states of the model. Further, the framework also calculates any potential separatrices dividing stable concentration regimes in multi-stable systems by integrating along negative time from an unstable steady state. If the dynamical model possesses multiple stable states, the framework then computes the time that would be required to switch between these states upon the addition of an effector molecule (e.g. IPTG, aTC in the case of the genetic toggle switch). Additionally, we coupled the continuity analysis capabilities of the PyDSTool[31] package in Python to our modeling framework to enable calculation of limit points (parameter values where the behavior of the model changes) and thereby determine stability regimes over parameter ranges for the dynamical system of interest. The framework has been packaged as a Python module is available on GitHub[32]. It uses functionalities from the scipy[33] and PyDSTool[31] packages of python[33].

6.3 Design and construction of DNA parts and plasmids

The RBS calculator (v2.1) proposed by Reis et al[19] was used to design constructs with varying translation initiation rates(TIRs) or strengths of the Ribosome Binding Sequence (RBS) and to calculate the RBS strengths of previously available constructs, where necessary. The genetic toggle switch constructed by Litcofsky et al[13] was used as the template to construct the fusion toggle switch, which was then used as the base plasmid for all further constructions. Unique Nucleotide Sequences (UNSs)[34] were added upstream and downstream of each genetic part to improve their modularity and enable rapid assembly of different combinations of genetic parts. Preliminary DNA parts for varying RBS's and protease affinity tags of the repressors were synthesized by Ranomics Inc. Synthetic oligonucleotide parts for DNA assembly reactions were synthesized by Eurofins Scientific and Integrated DNA Technologies Inc. Ligase Cycling Reaction (LCR)[29] and Gibson assembly[35] were used to assemble different DNA parts into complete plasmids. Plasmids were maintained in *E. coli* (DH10β) cells after assembly by transfection through heat shock or electroporation. An Opentrons robotic liquid handler was programmed to perform DNA and plasmid extractions where higher throughput was required. All PCR amplifications for plasmid construction were performed using Q5 High-Fidelity Polymerase (NEB). All plasmids were sequence verified through Sanger sequencing. *E. coli* cells harboring the target plasmids were stored in 20% glycerol at -80°C. Sequence files for plasmids used in this study can be found attached as supplementary files and are described in Table S5.

6.4 Characterization of fusion protein constructs and toggle switch variants

The constructed plasmids were transformed into *E. coli* (MG1655) Δ lacI - the target host for final characterization, through electroporation. All strains were characterized using an in-house microplate based high throughput robotic platform that has been previously described[30]. Cells were grown in microtiter plates overnight using LB media supplemented with 1% glucose and the appropriate inducer (2 mM isopropyl β-D-1-thiogalactopyranoside - IPTG or 500 ng/mL anhydrotetracycline - aTc). Following this, they were transferred to fresh Rich Defined Media with the same inducer, supplemented with 1% glucose and allowed to adapt to the new media overnight. Rich defined media (RDM) was used as the growth medium for phenotyping experiments. It is composed of a carbon source (D-glucose at various concentrations), salts (3.5 g/L KH_2PO_4, 5 g/L K_2HPO_4, 3.5 g/L $(NH_4)_2HPO_4$, 1 mM $MgSO_4$, 0.1mM $CaCl_2$), 1 mM 3-morpholinopropane-1-sulfonic acid (MOPS), amino acid supplements (0.8 mM alanine, 5.2 mM arginine, 0.4 mM aspargine, 0.4 mM aspartate, 0.1 mM cysteine, 0.6 mM glutamate, 0.6 mM glutamine, 0.8 mM glycine, 0.2 mM histidine, 0.4 mM isoleucine, 0.8 mM leucine, 0.4 mM lysine, 0.2 mM methionine, 0.4 mM phenylalanine, 0.4 mM proline, 10 mM serine, 0.4 mM threonine, 0.1 mM tryptophan, 0.2 mM tyrosine, and 0.6 mM valine), nucleotide supplements (0.1 mM each of adenine, cytosine, guanine, and uracil), and vitamin supplements (0.01 mM each of thiamine, calcium pantothenate, *p*-aminobenzoic acid, *p*-hydroxybenzoic acid, and 2,3-dihydroxybenzoic acid) - adapted from the defined media composition described previously[36].

To examine the speed of switching, overnight RDM cultures were then washed with RDM media without any inducer to remove traces of the previously used inducer and transferred to fresh rich defined media[36] at a uniform cell density corresponding to OD_{700} of 0.01. The required inducer (2 mM IPTG to strains grown overnight on aTc and 500 ng/mL aTC to strains grown overnight on IPTG) was added to the plates which were then incubated in a Tecan Spark microplate reader at 37°C. The cell densities and concentrations of reporter proteins were monitored by recording absorbance at 700 nm and fluorescence intensities using the following parameters: GFP (Excitation: 488 nm, Emission: 525 nm, Gain: 90), mCherry (Excitation: 570 nm, Emission: 610 nm, Gain: 110). For bi-stability tests, overnight cultures of *E. coli* in RDM containing the appropriate inducer were washed with media lacking inducer to remove all traces of the previously used inducer. Then, cells were inoculated in fresh RDM at a cell density of $OD_{700} = 0.01$ and grown to saturation. Following this, the cells were progressively transferred two more times to fresh media lacking inducer at a 1:100 dilution at 12 hour intervals, with the cell density and fluorescent reporter concentrations being recorded at the end of each transfer.

6.5 Data analysis

Blank subtracted fluorescence values normalized to the measured cell density values were used to track repressor protein levels in the cells. For the switch speed experiments, the time required to switch was calculated as the time taken for the fluorescent reporters to reach their steady state concentrations. This was done by approximating the first derivative of OD normalized fluorescence data and determining the time at which its absolute value becomes lower than a fixed threshold. For bi-stability analysis, the GFP and mCherry fluorescence at the end of each transfer was recorded. The cells were considered stable in their state if the fluorescence values of the corresponding reporter was at a detectable level after each of the three transfers, indicating that the corresponding repressor is also still at high levels. Individual replicates

were considered bi-stable if both states were stable at the end of three transfers and each toggle switch variant strain was considered bi-stable if all the individual replicates were bi-stable after three transfers. Data analyses for all sections were conducted using Python on Jupyter notebooks. The jupyter notebooks used to generate figures and process data in this work have been made available on GitHub[37]. The python based data analysis library - pandas and plotting library - plotly were used extensively for all data analysis and visualization pipelines in this work[38,39]. Microbial phenotypic data and growth curves were analyzed using the IMPACT framework[40].

Acknowledgements

This work was supported by the Natural Sciences and Engineering Research Council (NSERC), the NSERC Industrial Biocatalysis Network, the Ontario Ministry of Research and Innovation, and Genome Canada.

References

[1] Timo Hardiman, Karin Lemuth, Markus A. Keller, Matthias Reuss, and Martin Siemann-Herzberg. Topology of the global regulatory network of carbon limitation in Escherichia coli. *J. Biotechnol.*, 132(4):359–374, 2007.

[2] Joe Lutkenhaus. The regulation of bacterial cell division: A time and place for it. *Curr. Opin. Microbiol.*, 1(2):210–215, 1998.

[3] Andrea Pitzschke, Adam Schikora, and Heribert Hirt. MAPK cascade signalling networks in plant defence. *Curr. Opin. Plant Biol.*, 12(4):421–426, 2009.

[4] Uri Alon. Network motifs: Theory and experimental approaches. *Nat. Rev. Genet.*, 8(6):450–461, 2007.

[5] James E. Ferrell. Feedback regulation of opposing enzymes generates robust, all-or-none bistable responses. *Curr. Biol.*, 18(6):R244–R245, 2008.

[6] Timothy S. Gardner, Charles R. Cantor, and James J. Collins. Construction of a genetic toggle switch in Escherichia coli. *Nature*, 403(6767):339–342, 2000.

[7] Naveen Venayak, Kaushik Raj, Rohil Jaydeep, and Radhakrishnan Mahadevan. An Optimized Bistable Metabolic Switch to Decouple Phenotypic States during Anaerobic Fermentation. *ACS Synth. Biol.*, 7(12):2854–2866, oct 2018.

[8] William Bothfeld, Grace Kapov, and Keith E.J. Tyo. A Glucose-Sensing Toggle Switch for Autonomous, High Productivity Genetic Control. *ACS Synth. Biol.*, 6(7):1296–1304, jul 2017.

[9] David T. Riglar, Tobias W. Giessen, Michael Baym, S. Jordan Kerns, Matthew J. Niederhuber, Roderick T. Bronson, Jonathan W. Kotula, Georg K. Gerber, Jeffrey C. Way, and Pamela A. Silver. Engineered bacteria can function in the mammalian gut long-term as live diagnostics of inflammation. *Nat. Biotechnol.*, 35(7):653–658, may 2017.

[10] Jonathan W. Kotula, S. Jordan Kerns, Lev A. Shaket, Layla Siraj, James J. Collins, Jeffrey C. Way, and Pamela A. Silver. Programmable bacteria detect and record an environmental signal in the mammalian gut. *Proc. Natl. Acad. Sci. U. S. A.*, 111(13):4838–4843, 2014.

[11] Clement T.Y. Chan, Jeong Wook Lee, D. Ewen Cameron, Caleb J. Bashor, and James J. Collins. 'Deadman' and 'Passcode' microbial kill switches for bacterial containment. *Nat. Chem. Biol.*, 12(2):82–86, feb 2016.

[12] Finn Stirling, Lisa Bitzan, Samuel O'Keefe, Elizabeth Redfield, John W.K. Oliver, Jeffrey Way, and Pamela A. Silver. Rational Design of Evolutionarily Stable Microbial Kill Switches. *Mol. Cell*, 68(4):686–697.e3, nov 2017.

[13] Kevin D. Litcofsky, Raffi B. Afeyan, Russell J. Krom, Ahmad S. Khalil, and James J. Collins. Iterative plug-and-play methodology for constructing and modifying synthetic gene networks. *Nat. Methods*, 9(11):1077–1080, nov 2012.

[14] Jeong Wook Lee, Andras Gyorgy, D. Ewen Cameron, Nora Pyenson, Kyeong Rok Choi, Jeffrey C. Way, Pamela A. Silver, Domitilla Del Vecchio, and James J. Collins. Creating Single-Copy Genetic Circuits. *Mol. Cell*, 63(2):329–336, jul 2016.

[15] Kaushik Raj, Naveen Venayak, and Radhakrishnan Mahadevan. Novel two-stage processes for optimal chemical production in microbes. *Metab. Eng.*, 62:186–197, nov 2020.

[16] Jordan J. Sickle, Congjian Ni, Daniel Shen, Zewei Wang, Matthew Jin, and Ting Lu. Integrative Circuit-Host Modeling of a Genetic Switch in Varying Environments. *Sci. Rep.*, 10(1):1–9, may 2020.

[17] Rong Zhang, Jiao Li, Juan Melendez-Alvarez, Xingwen Chen, Patrick Sochor, Hanah Goetz, Qi Zhang, Tian Ding, Xiao Wang, and Xiao Jun Tian. Topology-dependent interference of synthetic gene circuit function by growth feedback. *Nat. Chem. Biol.*, 16(6):695–701, apr 2020.

[18] Stefan Klumpp, Zhongge Zhang, and Terence Hwa. Growth rate-dependent global effects on gene expression in bacteria. *Cell*, 139(7):1366–75, dec 2009.

[19] Alexander C. Reis and Howard M. Salis. An automated model test system for systematic development and improvement of gene expression models. *ACS Synth. Biol.*, 9(11):3145–3156, 2020.

[20] Kathleen E. McGinness, Tania A. Baker, and Robert T. Sauer. Engineering Controllable Protein Degradation. *Mol. Cell*, 22(5):701–707, 2006.

[21] David W. Erickson, Severin J. Schink, Vadim Patsalo, James R. Williamson, Ulrich Gerland, and Terence Hwa. A global resource allocation strategy governs growth transition kinetics of Escherichia coli. *Nature*, 551(7678):119, nov 2017.

[22] F.C. Neidhardt. *Escherichia Coli and Salmonella: Cellular and Molecular Biology.* Number v. 1-2 in Escherichia Coli and Salmonella: Cellular and Molecular Biology. ASM Press, 1996.

[23] Jia Xu and Kathleen S. Matthews. Flexibility in the inducer binding region is crucial for allostery in the Escherichia coli lactose repressor. *Biochemistry*, 48(22):4988–4998, jun 2009.

[24] Subhayu Basu, Yoram Gerchman, Cynthia H. Collins, Frances H. Arnold, and Ron Weiss. A synthetic multicellular system for programmed pattern formation. *Nature*, 434(7037):1130–1134, apr 2005.

[25] Jiunn R. Chen. Improving the speed of the genetic toggle switch without sacrificing its dynamic stability. *Phys. Rev. E - Stat. Nonlinear, Soft Matter Phys.*, 73(4):041901, apr 2006.

[26] Daniel Huang, William J. Holtz, and Michel M. Maharbiz. A genetic bistable switch utilizing nonlinear protein degradation. *J. Biol. Eng.*, 6(1):9, 2012.

[27] Xiaoying Chen, Jennica L. Zaro, and Wei Chiang Shen. Fusion protein linkers: Property, design and functionality. *Adv. Drug Deliv. Rev.*, 65(10):1357–1369, 2013.

[28] Jianshen Hou, Cong Gao, Liang Guo, Jens Nielsen, Qiang Ding, Wenxiu Tang, Guipeng Hu, Xiulai Chen, and Liming Liu. Rewiring carbon flux in Escherichia coli using a bifunctional molecular switch. *Metab. Eng.*, 61:47–57, 2020.

[29] Stefan De Kok, Leslie H. Stanton, Todd Slaby, Maxime Durot, Victor F. Holmes, Kedar G. Patel, Darren Platt, Elaine B. Shapland, Zach Serber, Jed Dean, Jack D. Newman, and Sunil S. Chandran. Rapid and reliable DNA assembly via ligase cycling reaction. *ACS Synth. Biol.*, 3(2):97–106, 2014.

[30] Kaushik Raj, Naveen Venayak, Patrick Diep, Sai Akhil Golla, Alexander F. Yakunin, and Radhakrishnan Mahadevan. Automation assisted anaerobic phenotyping for metabolic engineering. *Microb. Cell Fact.*, 20(1):1–16, 2021.

[31] Robert Clewley. Hybrid models and biological model reduction with pydstool. *PLOS Computational Biology*, 8(8):1–8, 08 2012.

[32] Kaushik Raj, William T Z Wong, Beini Zhang, and Radhakrishnan Mahadevan. Novel dynamical modeling framework GitHub repository. Available from: `https://github.com/LMSE/dynaCA`. Accessed 10 July 2022, 2022.

[33] Pauli Virtanen, Ralf Gommers, Travis E. Oliphant, Matt Haberland, Tyler Reddy, David Cournapeau, Evgeni Burovski, Pearu Peterson, Warren Weckesser, Jonathan Bright, Stéfan J. van der Walt, Matthew Brett, Joshua Wilson, K. Jarrod Millman, Nikolay Mayorov, Andrew R.J. Nelson, Eric Jones, Robert Kern, Eric Larson, C. J. Carey, İlhan Polat, Yu Feng, Eric W. Moore, Jake VanderPlas, Denis Laxalde, Josef Perktold, Robert Cimrman, Ian Henriksen, E. A. Quintero, Charles R. Harris, Anne M. Archibald, Antônio H. Ribeiro, Fabian Pedregosa, Paul van Mulbregt, Aditya Vijaykumar, Alessandro Pietro Bardelli, Alex Rothberg, Andreas Hilboll, Andreas Kloeckner, Anthony Scopatz, Antony Lee, Ariel Rokem, C. Nathan Woods, Chad Fulton, Charles Masson, Christian Häggström, Clark Fitzgerald, David A. Nicholson, David R. Hagen, Dmitrii V. Pasechnik, Emanuele Olivetti, Eric Martin, Eric Wieser, Fabrice Silva, Felix Lenders, Florian Wilhelm, G. Young, Gavin A. Price, Gert Ludwig Ingold, Gregory E. Allen, Gregory R. Lee, Hervé Audren, Irvin Probst, Jörg P. Dietrich, Jacob Silterra, James T. Webber, Janko Slavič, Joel Nothman, Johannes Buchner, Johannes Kulick, Johannes L. Schönberger, José Vinícius de Miranda Cardoso, Joscha Reimer, Joseph Harrington, Juan Luis Cano Rodríguez, Juan Nunez-Iglesias, Justin Kuczynski, Kevin Tritz, Martin Thoma, Matthew Newville, Matthias Kümmerer, Maximilian Bolingbroke, Michael Tartre, Mikhail

Pak, Nathaniel J. Smith, Nikolai Nowaczyk, Nikolay Shebanov, Oleksandr Pavlyk, Per A. Brodtkorb, Perry Lee, Robert T. McGibbon, Roman Feldbauer, Sam Lewis, Sam Tygier, Scott Sievert, Sebastiano Vigna, Stefan Peterson, Surhud More, Tadeusz Pudlik, Takuya Oshima, Thomas J. Pingel, Thomas P. Robitaille, Thomas Spura, Thouis R. Jones, Tim Cera, Tim Leslie, Tiziano Zito, Tom Krauss, Utkarsh Upadhyay, Yaroslav O. Halchenko, and Yoshiki Vázquez-Baeza. SciPy 1.0: fundamental algorithms for scientific computing in Python. *Nat. Methods*, 17(3):261–272, 2020.

[34] Joseph P. Torella, Florian Lienert, Christian R. Boehm, Jan Hung Chen, Jeffrey C. Way, and Pamela A. Silver. Unique nucleotide sequence-guided assembly of repetitive DNA parts for synthetic biology applications. *Nat. Protoc.*, 9(9):2075–2089, 2014.

[35] Daniel G. Gibson, Lei Young, Ray Yuan Chuang, J. Craig Venter, Clyde A. Hutchison, and Hamilton O. Smith. Enzymatic assembly of DNA molecules up to several hundred kilobases. *Nat. Methods*, 6(5):343–345, may 2009.

[36] F. C. Neidhardt, P. L. Bloch, and D. F. Smith. Culture medium for enterobacteria. *J. Bacteriol.*, 119(3):736–747, 1974.

[37] Kaushik Raj, William T Z Wong, Beini Zhang, and Radhakrishnan Mahadevan. Enhanced bistable motifs GitHub repository. Available from: `https://github.com/LMSE/enhanced_bistable_switches`. Accessed 10 July 2022, 2022.

[38] Pandas Development team. pandas-dev/pandas: Pandas, feb 2020.

[39] Plotly Technologies Inc. Collaborative data science, 2015.

[40] Naveen Venayak, Kaushik Raj, and Radhakrishnan Mahadevan. Impact framework: A python package for writing data analysis workflows to interpret microbial physiology. *Metab. Eng. Commun.*, 9, 2019.